Environmental Science & Technology

pubs.acs.org/est

Article

Spatial and Temporal Resolution of Cyanobacterial Bloom Chemistry Reveals an Open-Ocean *Trichodesmium thiebautii* as a Talented Producer of Specialized Metabolites

Christopher W. Via,◆ Laura Grauso,◆ Kelly M. McManus, Riley D. Kirk, Andrew M. Kim, Eric A. Webb, Noelle A. Held, Mak A. Saito, Silvia Scarpato, Paul V. Zimba, Peter D. R. Moeller, Alfonso Mangoni,* and Matthew J. Bertin*

Cite This: *Environ. Sci. Technol.* 2024, 58, 9525−9535

Read Online

ACCESS | Metrics & More | Article Recommendations | Supporting Information

ABSTRACT: While the ecological role that *Trichodesmium* sp. play in nitrogen fixation has been widely studied, little information is available on potential specialized metabolites that are associated with blooms and standing stock *Trichodesmium* colonies. While a collection of biological material from a *T. thiebautii* bloom event from North Padre Island, Texas, in 2014 indicated that this species was a prolific producer of chlorinated specialized metabolites, additional spatial and temporal resolution was needed. We have completed these metabolite comparison studies, detailed in the current report, utilizing LC-MS/MS-based molecular networking to visualize and annotate the specialized metabolite composition of these *Trichodesmium* blooms and colonies in the Gulf of Mexico (GoM) and other waters. Our results showed that *T. thiebautii* blooms and colonies found in the GoM have a remarkably consistent specialized metabolome. Additionally, we isolated and characterized one new macrocyclic compound from *T. thiebautii*, trichothilone A (**1**), which was also detected in three independent cultures of *T. erythraeum*. Genome mining identified genes predicted to synthesize certain functional groups in the *T. thiebautii* metabolites. These results provoke intriguing questions of how these specialized metabolites affect *Trichodesmium* ecophysiology, symbioses with marine invertebrates, and niche development in the global oligotrophic ocean.

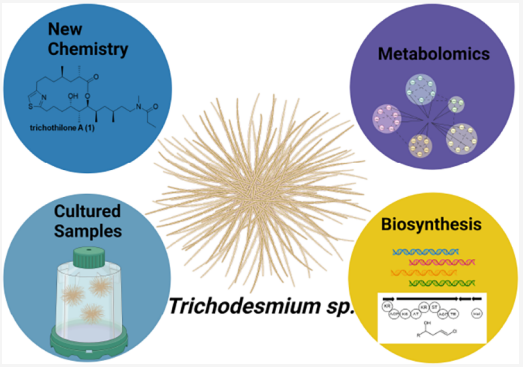

KEYWORDS: *cyanobacterial blooms, mass spectrometry, molecular networking, specialized metabolites, Trichodesmium*

INTRODUCTION

As climate change results in both increased global temperatures and CO_2 concentrations in ocean waters, species of the cyanobacterial genus *Trichodesmium* are projected to expand their already substantial, oligotrophic ocean range as the subtropics move poleward.[1−3] An increase in oceanic and coastal growth of the periodically bloom-forming *Trichodesmium* will raise both the direct and indirect exposure risk to humans from potential toxins produced by this genus. While the ecological role of *Trichodesmium* as nitrogen fixers is well studied, the specialized metabolism of the genus along with the impact of potential toxins on human health and animal health is unknown. The latter is of increasing importance because of the aforementioned range and abundance expansions predicted for *Trichodesmium*.

Many aspects of *Trichodesmium*'s toxicity have been somewhat enigmatic and inconsistent. Multiple classes of metabolites and toxins have been identified from *Trichodesmium* blooms and environmental collections such as saxitoxin, microcystin, trichamide, and palytoxin.[4−8] Previous *Trichodesmium* toxicity studies performed using homogenized cells, filtrates, aging cells, and crude extracts of *Trichodesmium thiebautii* have shown toxicity to copepod grazers, while those from *Trichodesmium erythraeum* did not show the same levels of toxicity.[9,10] However, extracts of *T. erythraeum* samples obtained from coastal India showed toxicity to shrimp and multiple human cell lines.[11] This previous work has not included metabolite analysis of repeated field collections, biosynthetic gene cluster information, and culture confirmations, which has made interpreting toxicity studies challenging.

To address this gap, we completed an integrative, systematic study of the metabolites produced by *Trichodesmium* species in the environment and from isolates in culture. Our previous work characterized *T. thiebautii* metabolites that represented new analogs from existing cytotoxic compound classes (e.g.,

Received: December 21, 2023
Revised: May 1, 2024
Accepted: May 3, 2024
Published: May 17, 2024

smenamides C, D, and E)[12] and new classes of cytotoxic metabolites (e.g., the trichophycins, tricholides, and trichothiazoles), which had not been described previously.[13−23]

In the current report, we detailed the results of continued field studies in 2017, 2019, and 2021 in the GoM to provide additional temporal and spatial resolution of specialized metabolite production. The culmination of these studies has shown that these metabolites can be detected in *T. thiebautii* colonies year after year and throughout the GoM. We have used genetic tools to determine the *Trichodesmium* species present in these collections and untargeted MS/MS-based molecular networking to provide a chemical inventory of colony and bloom metabolites. It appears clear from our data that *T. thiebautii* in the oligotrophic GoM is a prolific producer of specialized metabolites, many of which possess nanomolar cytotoxicity against human cells (certain smenamides and smenothiazoles).[17,18] We report a new metabolite in this work, trichothilone A (**1**), which was confirmed in multiple *Trichodesmium* laboratory cultures. Additionally, we identified key genetic architecture in the *T. thiebautii* H94 genome that is consistent with the generation of key functional groups in many of the metabolites we have characterized, i.e., the chlorovinylidene group and terminal vinyl chloride present in the trichophycins and smenolactones, the trichotoxins, the smenamides, the conulothiazoles, and trichothiazole A.[12−16,19−23] This study provokes intriguing questions with respect to the full chemical potential of the members of this genus.

MATERIALS AND METHODS

Collection of Cyanobacteria, Genetic Analysis, and Extraction Procedures. *Trichodesmium* biomass was collected from the Gulf of Mexico near North Padre Island, Texas, in 2014. As described previously, the dominant organism was identified as *Trichodesmium* sp., and the material was shipped to our laboratory.[13,24] The biomass (14 g dry weight) was repeatedly extracted with a 2:1 mixture of CH_2Cl_2:CH_3OH, and the crude extract was concentrated to an oil under reduced pressure. Collections were also made from the GoM in 2017, 2019, and 2021. Select samples were preserved in RNAlater and transferred to the laboratory. DNA isolation, PCR amplification of 16S rRNA genes, and phylogenetic analysis followed the procedures of McManus and co-workers exactly.[23] 16S rRNA sequences have been deposited in NCBI GenBank (GoM2017 accession no. OR661266; GoM2019-11 accession no. OR665426). Additionally, samples were acquired from the TriCoLim 2018 expedition[25] and from culture collections (Table S1). The biomass from each of these sites was extracted in 2:1 CH_2Cl_2:CH_3OH, followed by a 1:1 CH_2Cl_2:CH_3OH, and 100% CH_3OH. The resulting crude extracts were separately concentrated to oils under reduced pressure. Small aliquots of the resulting crude extracts were passed over a 100 mg C18 SPE column to prepare for LC-MS/MS analysis. Trichothilone A (**1**) was isolated from 2014 and 2019 extracts, and information on the isolation and physical characteristics of the molecule can be found in the Supporting Information.

LC-MS/MS-Based Molecular Networking. The resulting extracts described above were analyzed on a liquid chromatography system, a Dionex UltiMate 3000 HPLC, coupled to a high-resolution electrospray mass spectrometer, a Thermo LTQ Orbitrap XL system with postacquisition analysis performed at the GNPS Web site.[26] All raw mass spectrometry files and .mzXML files can be found in the Center for Computational Mass Spectrometry MassIVE repository under number MSV000093069. For LC-MS/MS methodological details, please refer to the Supporting Information.

Cytotoxicity Assays. Assays were carried out as previously described using neuro-2A cells.[13] Compound **1** was dissolved in DMSO (1% v/v) and added to the cells in the range of 100 to 0.1 μM in order to generate EC_{50} curves against both cell lines. Four technical replicates were prepared for each concentration, and each assay was performed in triplicate. Doxorubicin was used as a positive control, and DMSO (1% v/v) was used as a negative control.

Genomic Analysis. The *T. erythraeum* IMS101 assembled genome sequence was retrieved from the European Nucleotide Archive (accession #CP000393). The *T. thiebautii* H94 genome and a group of field sample metagenome-assembled genome (MAG) assemblies were retrieved from NCBI's SRA (BioProject PRJNA828267).[25]

RESULTS

Morphological Analysis and DNA Sequencing of Organism Collections. Our previous work from an initial collection of *T. thiebautii* biomass near North Padre Island, Texas, in 2014 provided the first evidence that there was a *Trichodesmium* species capable of prolific specialized metabolite production in the GoM. Mining this biomass resulted in the characterization of 24 new molecules,[12−16,19−23] including **1** presented in the current report. Additionally, seven chlorinated metabolites were detected from the 2014 collection via analysis of LC-MS/MS molecular networks. These metabolites were originally isolated and characterized from the sponge *Smenospongia aurea* but putatively considered as the products of associated cyanobacteria due to the chlorovinylidene functional group present in these metabolites.[17,18,20−22]

The primary purpose of the current work was to determine if metabolite composition of these *T. thiebautii* colonies in the GoM was consistent over time and geographic location. To accomplish this, a second collection of *Trichodesmium* colonies was made in the GoM (27.00° N; 92.00° W) in 2017 (GoM2017, Table S1). Additionally in 2019, aboard the R/V Oregon II (National Oceanic and Atmospheric Administration), we visited several stations in the GoM and collected *Trichodesmium* colonies and biomass (GoM 2019-2-4, 6, 11, Table S1 and Figure S1). Collections from 2017 and 2019 were identified as predominantly *Trichodesmium* sp. by examining filaments and puff and tuft colonies (Figure S2). Phylogenetic analysis of partial sequences of the 16S rRNA gene supported identification of samples as *T. thiebautii* (GoM2017, GoM2019-11), clustering with the *T. thiebautii* identified in the 2014 collection (Figure 2B). During the 2019 research cruise, we collected bulk biomass from a surface accumulation (GoM2019-6) and were also able to harvest individual tuft and puff colonies from certain stations, sequestering individual colonies with a sterile loop and preserving them for laboratory analysis (e.g., GoM2019-11) (Figure S3). More field samples were collected from the GoM in 2021 (GoM2021-2-4, Table S1), and three cultivated samples of *T. erythraeum* IMS101 were examined—two separate cultures obtained from the Bigelow Laboratory for Ocean Sciences (IMS101) and another from the University of Southern California *Trichodesmium* Culture Collection (USCTCC) (*T. erythraeum* ST8) (Table S1). Finally, we examined legacy samples from a 2018 TriCoLim research expedition (AT39-05) in the Caribbean and Atlantic Ocean (TriCoLim St 3, 4, 6, 8, 13, 15, 16, 17, 20) (Table S1), which

https://doi.org/10.1021/acs.est.3c10739
Environ. Sci. Technol. 2024, 58, 9525−9535

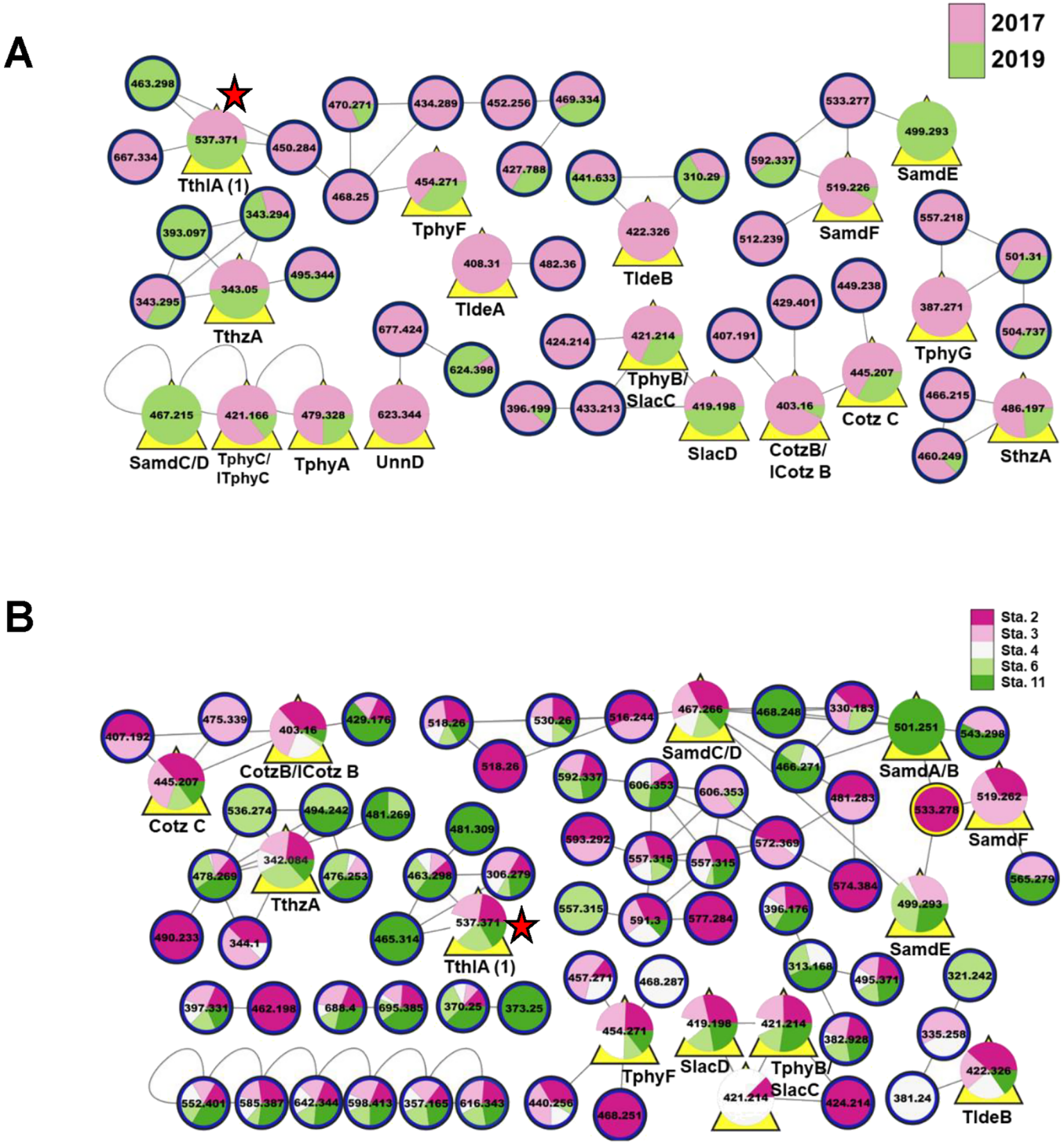

Figure 1. *T. thiebautii* specialized metabolites were found year after year and across the GoM. (A) Partial LC-MS/MS-based molecular network of extracts from collection GoM2017 (pink) and GoM2019-6 (green). (B) *T. thiebautii* specialized metabolites found across the GoM in 2019. Partial LC-MS/MS-based molecular network of extracts from 2019 collections (stations 2−4, 6, and 11). In all panels, nodes are designated by their precursor masses. In panels (A) and (B), yellow triangles behind the node indicate that these metabolites were previously characterized by our group (cf. Figure S4). In panel (B), "pie slices" designate stations where the metabolite was detected. Red stars show the position of the node for trichothilone A (**1**) (*m*/*z* 537). Cotz, conulothiazole; ICotz, isoconulothiazole; ITphy, isotrichophycin; Sam, smenamide; Slac, smenolactone; Sthz, smenothiazole; Tlde, tricholide; Tphy, trichophycin; Tthl, trichothilone; Tthz, trichothiazole; Unn, unnarmicin. The full networks can be found at http://gnps.ucsd.edu/ProteoSAFe/status.jsp?task = 27cc1b6493804e0283a08d5d056d015d (temporal−total number of nodes in full network 1465), http://gnps.ucsd.edu/ProteoSAFe/status.jsp?task=4b5821e25366435fae44da433db8819e (spatial—total number of nodes in full network 538).

expanded the geographic coverage of metabolite composition of *Trichodesmium* colonies outside of the GoM. Collections and cultures used in this study are summarized in Table S1.

LC-MS/MS-Based Molecular Networking: Spatial and Temporal Resolution of *Trichodesmium* Metabolites. We utilized LC-MS/MS paired with molecular networking to

https://doi.org/10.1021/acs.est.3c10739
Environ. Sci. Technol. 2024, 58, 9525−9535

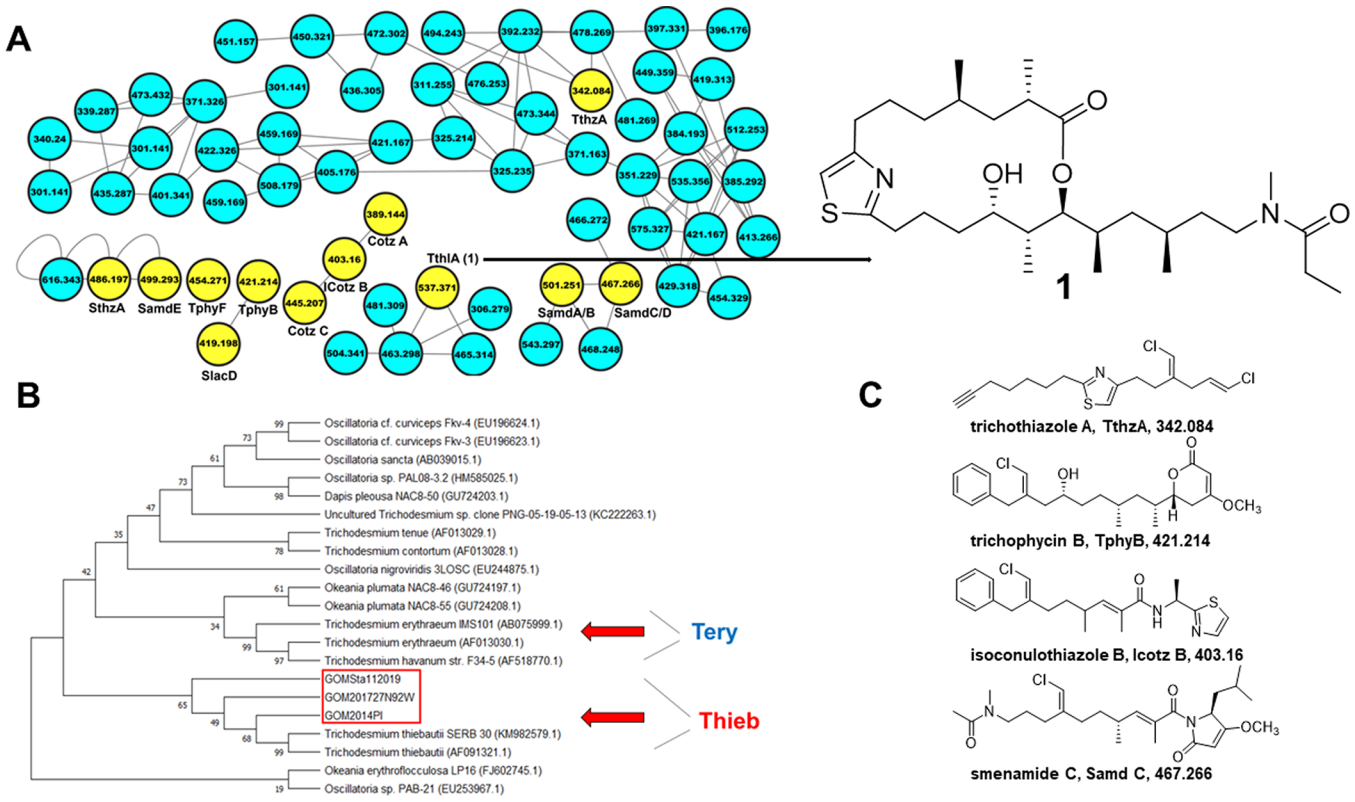

Figure 2. (A) *T. thiebautii* specialized metabolites in "picked colonies". Partial LC-MS/MS-based molecular network of extract from GoM2019-11. Colonies were hand-picked with a sterile loop from bulk collection, and an extract was generated. An arrow points from node *m*/*z* 537 (ThlA) to the trichothilone A (**1**) structure. Yellow nodes in panel (A) indicate that these metabolites were previously characterized by our group (cf. Figure S4). The full network can be found at http://gnps.ucsd.edu/ProteoSAFe/status.jsp?task=9b6cefbe17c44ecf897caec9aba38031 (picked colonies−total number of nodes 241). (B) 16S rRNA phylogenetic tree aligning *Trichodesmium* species from this study (red box—PI2014, GoM 2017, and GoM2019-11). All samples clustered with *T. thiebautii*. The tree was created using the Maximum Likelihood method and the Tamura-Nei model. The bootstrap consensus tree is inferred from 1000 replicates, and the percentage of replicate trees in which the associated taxa clustered together in the bootstrap test are shown next to branches. Analysis was conducted in MEGA. GenBank accession numbers of sequences are noted in parentheses. Red arrows show clusters for *T. erythraeum* (Tery) and *T. thiebautii* (Thieb). (C) Representative structures that have been characterized from *Trichodesmium* collections previously and were found in the "picked colonies" molecular network with their names, abbreviations, and *m*/*z* values below the structures.

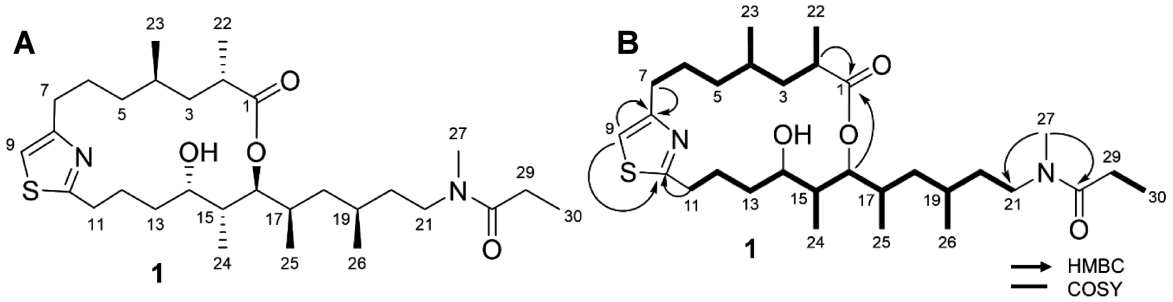

Figure 3. Structure of trichothilone A (**1**) (left) and key 2D NMR correlations (right).

compare the metabolite composition of *Trichodesmium* collections over time and geographic area in the GoM. The previously characterized metabolites from the 2014 collection served as a "screening library" for specialized metabolites (Figure S4). Collections from 2017 and 2019 showed remarkable consistency with respect to metabolite content when compared to the previous 2014 analysis. Several of the previously characterized metabolites from the 2014 collection were identified in samples from 2017 (21 metabolites annotated) and 2019 (18 metabolites annotated). These include many of the trichophycins, smenamides, tricholides, trichothiazoles, conulothiazoles, smenothiazole A, and trichothilone A (**1**) (Figure 1A).

Examining by geographic location using the 2019 samples, we again annotated many of the previously characterized metabolites from 2014 including trichophycins B and F, smenolactones C and D, smenamides A-F, isoconulothiazole B and conulothiazole C, trichothiazole A, tricholide B, and **1**. There were also over 25 metabolites that remain unidentified but were detected from all five stations (Figure 1B).

We next analyzed the sample GoM2019-11, composed of "picked" colonies (dominated by puff morphology). These colonies were collected via net tow, washed in a sieve, and

https://doi.org/10.1021/acs.est.3c10739
Environ. Sci. Technol. 2024, 58, 9525−9535

Table 1. NMR Data for Trichothilone A (1)[a] in DMSO-d_6 (500 MHz for ^{1}H NMR, 125 MHz for ^{13}C NMR)

position	δ_C, type	δ_H (J in Hz)	HMBC	COSY
1	175.5, C			
2	35.5, CH	2.44, ovlp[b]	1, 3, 22	22, 3a, 3b
3a	40.0, CH_2	1.32, m	2, 4, 22, 23	2, 4
3b		1.16, m	2, 4, 22, 23	2, 4
4	29.1, CH	1.42, ovlp	3, 5, 6, 23	3b, 5, 23
5	34.9, CH_2	1.06, ovlp	6, 23	4, 6a, 6b
6a	25.0, CH_2	1.70, m		5, 7a, 7b
6b		1.59, m		5, 7a
7a	29.9, CH_2	2.73, m	6, 8	6b
7b		2.49, m		6a
8	156.0, C			
9	112.8, CH	7.01, s	8, 10	
10	169.1, C			
11a	31.2, CH_2	2.96, ddd (14.9, 6.7, 3.8)	10, 13	12
11b		2.77, m	10, 13	12
12	26.0, CH_2	1.75, m		11a, 11b, 13a, 13b
13a	32.5, CH_2	1.40, ovlp		12, 14
13b		1.13, ovlp		12, 14
14	68.9, CH	3.18, m		13a, 13b, 15, OH
OH		4.19, br		14
15	38.8, CH	1.51, p (7.0)	16, 24	16, 24
16	76.7, CH	4.81, ddd (9.5, 7.2, 2.5)	1, 25	15, 17
17	30.5, CH	1.80, m		
16, 18, 25				
18	41.0, CH_2	1.01, m	17, 19, 25, 26	17, 19
19	26.9, CH	1.42, ovlp		18, 26
20a	34.2, CH_2	1.38, ovlp	19, 26	19, 21
20b		1.19, ovlp	19, 21, 26	19, 21
21	44.5, CH_2	3.25, t (7.4)	19, 20, 28	20a, 20b
22	16.4, CH_3	1.01, d (6.8)	1, 2, 3	2
23	19.9, CH_3	0.81, d (6.8)	3, 4, 5	4
24	9.4, CH_3	0.71, ovlp	14, 15	15
25	12.3, CH_3	0.73, ovlp	16, 17, 18	17
26	19.3, CH_3	0.80, d (6.8)	18, 19, 20	19
27	34.3, CH_3	2.88, s	21, 28	
28	172.1, C			
29	25.8, CH_2	2.24, m	28, 30	30
30	9.2, CH_3	0.94, t (7.4)	28, 29	29

[a]Z-conformer chemical shift values. [b]Overlapping signals.

transferred one by one to a preservation vial using a sterile loop. This sample does have associated bacteria in it, but it is devoid of other phytoplankton and loosely associated ectocommensals, which was verified by microscopy. Many of the previously characterized metabolites were identified in this sample as well (2A,C). These results point to the existence of a core metabolome possessed by resident *T. thiebautii* colonies in the GoM, which has never been documented previously. This species produces hundreds of small organic metabolites, many of which are hallmarked by the incorporation of at least one halogen atom, typically chlorine (Figure S4). Following examination of all networks, one unidentified metabolite was prioritized for isolation and structure elucidation—m/z 537. This molecule was found in samples from 2014, 2017, all 2019 samples, and in the "picked colonies" sample. Additionally, ion counts obtained from LC-MS/MS indicated that this molecule was abundant in all samples. In contrast to most *T. thiebautii* metabolites, mass spectrometry analysis indicated that **1** did not contain any halogen atoms. Following the metabolite composition analysis, HPLC-DAD- and LC-MS-guided isolations were performed.

Structure Characterization of 1. HPLC-DAD and mass spectrometry-guided isolation resulted in the isolation of an optically active pale yellow oil (**1**) (Figure 3A). HRESIMS analysis of **1** gave a protonated molecule $[M + H]^+$ of m/z 537.3725 suggesting a molecular formula of $C_{30}H_{52}N_2O_4S$ and a requirement of six degrees of unsaturation (Figure S5). Examination of 1D and 2D NMR data (Figures S6−S11) were used to establish the planar structure of the molecule. Certain ^{1}H NMR resonances, most notably the *N*-methyl singlet, were split into two signals in a ratio of about 1:1. This suggested two conformers at the amide bond, which are detailed in Figure S12. The text discusses only the *Z*-conformer. This phenomenon has been described for other metabolites from *Trichodesmium* that contain an *N*-methyl amide functionality.[12] Inspection of the COSY spectrum and ^{1}H−^{1}H spin systems allowed for the assignment of three partial structures: the first from H-2 to H_2-7 including the 1,3-dimethyl system from C-1 to C-5, and a second from H_2-11 to H_2-21 including a 1,3,5-trimethyl system from C-

https://doi.org/10.1021/acs.est.3c10739
Environ. Sci. Technol. 2024, 58, 9525−9535

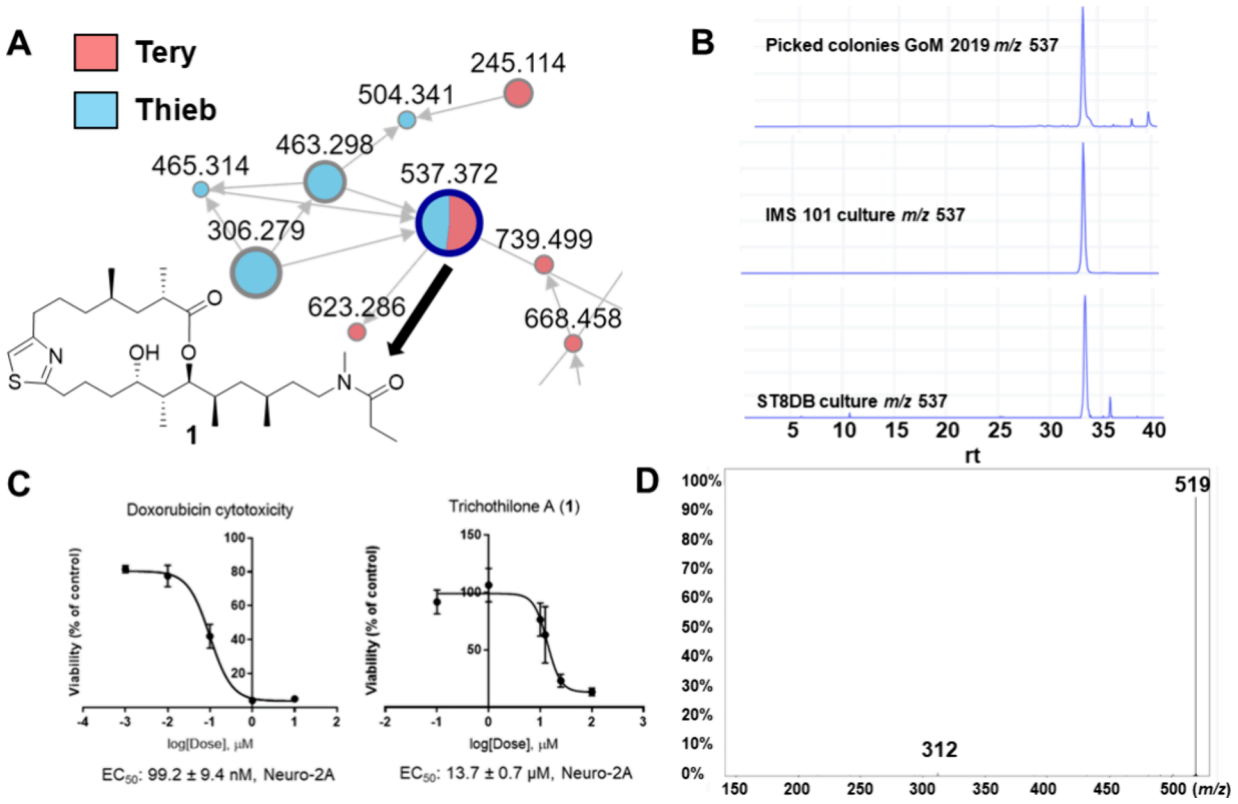

Figure 4. (A) Molecular network of extracts from GoM2019-11 and IMS101 and ST8 showing the trichothilone A (**1**) node present in both species. (B) Extracted ion chromatogram (XIC) shows detection of **1** in *T. erythraeum* IMS101 and ST8 extracts. (C) Cytotoxicity of **1** compared to the positive control doxorubicin against neuro-2A murine neuroblastoma cells. (D) MS/MS spectrum of trichothilone A (**1**).

14 to C-20 (Figure 3B). A third partial structure consisted of a single COSY correlation between H_3-30 and H_2-29. HMBC correlations between H_2-7 and C-8 (δ_C 156.0) and H_2-11 and C-10 (δ_C 169.1) along with the H-9 resonance (δ_H 7.01) established a thiazole functionality that connected the first two partial structures. An *N*-methyl signal (δ_H 2.88) showed HMBC correlations to C-21 (δ_C 44.5) and C-28 (δ_C 172.1) and connected partial structure two to an *N*-methylpropanamide functionality. HMBC correlations of H-2 (δ_H 2.44) and H-16 (δ_H 4.81) with C-1 (δ_C 175.5) established the ester of a macrolactone and satisfied the final degree of unsaturation characterizing a hybrid polyketide−peptide metabolite that was named trichothilone A (**1**) (Table 1).

Relative Configuration of 1. Relative configuration of the four stereogenic centers, C-14 to C-17, was determined as 14*S**,15*R**,16*S**,17*R** using the Murata's approach,[27] which is based on $^1H-^1H$ and $^1H-^{13}C$ scalar couplings and NOE effects, as detailed in Figure S13. The $^1H-^{13}C$ scalar couplings were directly measured using a HECADE-HSQC experiment (Figure S13)[28] or estimated as "large" or "small" from the ratio of the relative magnitudes of their cross peak measured in the HMBC spectrum with respect to a common proton, an intense peak indicating a large $^{2,3}J_{CH}$, a weak or missing peak a small $^{2,3}J_{CH}$.[29] Further support to the configuration of the segments C-14 to C-17 of **1** was provided by Kishi's method for the relative configuration of contiguous propionate units.[30,31] Comparison of ^{13}C NMR signals in **1** recorded in three different solvents ($CDCl_3$, CD_3OD, and DMSO-d_6) to Kishi's ^{13}C NMR database determined the relative configuration as $\alpha,\alpha,\beta,\beta$ for this segment (cf. Table S2 and Figure S14), fully confirming the stereochemical assignment based on Murata's method.

Determination of the relative configuration at C-2 and C-4 in **1** with respect to the C-14/C-17 segment was achieved using quantum-mechanical computational chemistry, namely, DFT prediction of ^1H and ^{13}C NMR chemical shifts (DFT-NMR).[32] Considering the structural complexity of compound **1**, the truncated model compound **1m** was used for the calculations, in which the flexible side chain of the natural compound is replaced by an isopropyl group. This strongly reduced the number of low-energy conformations of the molecule, while it did not significantly affect the chemical shifts of the region of the molecule under study.[33] The four possible stereoisomers of **1m** at C-2 and C-4 (*RR*-**1m**, *RS*-**1m**, *SR*-**1m**, *SS*-**1m**) were considered in the calculations (Figure S15). Conformational analysis of the four **4m** stereoisomers was performed using the program Pcmodel 10.0 (GMMX algorithm, MMFF94 force field),[34] which generated 35 through 66 conformers for each stereoisomer within 4 kcal/mol from the lowest-energy conformer (see SI Experimental Procedures for details).

All the conformers were optimized by DFT minimization using the Gaussian program at the B3LYP/6-31G(d,p)/SMD level,[35] and their ^1H and ^{13}C chemical shifts were calculated at the mPW1PW91/6-311+G(d,p)/PCM level. Average chemical shifts over all the conformers were then calculated for each of *RR*-**1m**, *RS*-**1m**, *SR*-**1m**, and *SS*-**1m** based on the Boltzmann distribution and compared with the experimental values measured for **1**. Comparison of the root-mean-square deviations (RMSD) of ^{13}C and ^1H chemical shifts immediately showed that *SR*-**1m** fit experimental data much better than the other three stereoisomers (*RR*-**1m**: 2.32 and 0.150 ppm; *RS*-**1m**: 2.24 and 0.145 ppm; *SR*-**1m**: 1.98 and 0.122 ppm; *SS*-**1m**: 2.46 and 0.149 ppm, respectively). The DP4+ statistical analysis of computa-

https://doi.org/10.1021/acs.est.3c10739
Environ. Sci. Technol. 2024, 58, 9525−9535

tional results fully confirmed this,[36] in that it assigned 100.00% probability to *SR*-**1m** being the correct stereoisomer (Figure S16). The *anti* orientation of the methyl groups at CH_3-22 and CH_3-23 of **1** determined above was further supported by the $\Delta(H_a-H_b)$ value (0.16 ppm) of the methylene protons attached to C-3, which is consistent with the trend shown for 1,3-*anti* dimethyl groups in the macrocycle myxovirescin (*anti* = 0.20 ppm; *syn* = 0.70 ppm).[37] Therefore, the relative configuration of **1** was extended to 2*S**,4*R**,14*S**,15*R**,16*S**,17*R** and only configuration at C-19 remained to be determined.

An attempt to determine the relative configuration at C-19 using DFT-NMR was unsuccessful because the predicted chemical shifts of the two possible epimers showed similar agreement with experimental data, with DP4+ probability <80% and therefore not conclusive (data not shown). Moreover, the $\Delta(H_a-H_b)$ value of the methylene protons attached to C-18, which was close to 0, could not be used for determination of relative configuration of the 1,3-dimethyl system CH_3-25/CH_3-26 because the method is unreliable when the methyl branches are adjacent to a lactone, which is the case for this system in **1**.[37] To overcome this limitation, we generated the acyclic methyl ester of **1**, characterized this derivative (**2**) using HRMS and ^{1}HNMR (Figures S17 and S18), and reanalyzed this compound to determine the chemical shifts of the intervening methylene unit in the 1,3-dimethyl system. The $\Delta(H_a-H_b)$ value of the methylene protons attached to C-18 of **2** ($\Delta(H_a - H_b) = 0.43$) strongly supported a *syn* relative configuration for CH_3-25 and CH_3-26 (Figure S14).[37] In addition, the $\Delta(H_a-H_b)$ measured for **2** was almost identical to the value (0.40 ppm) measured for the methylene protons attached to C-5 of the 4-bromophenacyl derivative of hemibourgeanic acid (**3**),[38] thus ruling out the possibility that the stereogenic centers C-16 and C-15 could affect the reliability of the method (Figure S19). These data defined the full relative configuration of **1** as 2*S**,4*R**,14*S**,15*R**,16*S**,17*R**,19*S**.

Absolute Configuration Analysis of 1. A single secondary alcohol in **1** (attached to C-14) allowed us to generate Mosher esters at that position. We analyzed the *S* and *R* esters of **1** via ^{1}H NMR, COSY, and TOCSY. A positive $\Delta(\delta_H S-\delta_H R)$ value for H-14 and negative $\Delta(\delta_H S-\delta_H R)$ values for H-9 and H-11 supported a 14*S* configuration (Figure S20). Relaying stereochemical assignments based on the previously determined relative configuration supported a 2*S*,4*R*,14*S*,15*R*,16*S*,17*R*,19*S* configuration of **1**.

Specialized Metabolites in Cultures and from Collections in the Wider Caribbean and Atlantic Ocean. Trichothilone A (**1**) was detected in both the cultivated *T. erythraeum* IMS101 samples and the *T. erythraeum* ST8 sample with matches to retention time, high-resolution mass spectrometry measurement, and MS/MS fragmentation pattern (Figure 4A,B,D). An examination of the cell mass and media of a second IMS101 culture also showed the presence of trichothilone A (**1**) (Figure S21), and its presence in the media may be related to its ecological relevance. Examining collections from the GoM collected aboard NOAA's R/V Oregon II in 2021 (revisiting stations from 2019) and samples from the TriCoLim expedition,[25] we continued to identify the presence of metabolites from our 2014 library by matching MS/MS fragmentation patterns. The GoM samples showed the presence of certain trichophycins, smenamides, and other molecules (Table S3). We detected trichothiazole A in extracts from TriCoLim stations 3, 8, 16, and 17 (Figure S22) and trichophycin F in 3, 6, and 17 (Figure S23). We also detected smenamide A/B from station 3 extracts (Figure S24).

Cytotoxicity of 1. Trichothilone A (**1**) showed modest cytotoxicity against neuro-2A cells with an IC_{50} value of 13.7 μM (Figure 4C). Due to the limited amount remaining following chemical degradation and derivative formation experiments, we were not able to investigate other bioactivities that the molecule might possess. The structural similarity of **1** to the thuggacins A and B, macrolactone antibiotics which showed biological activity against *Mycobacterium tuberculosis*,[39] provides optimism that additional testing of trichothilone A (**1**) could uncover potent therapeutically relevant biological activity.

Genomic Analysis of *T. thiebautii* H94, *T. erythraeum* IMS101, and Field Metagenomes. We examined several genome and MAGs that were publicly available,[25] searching for genetic architecture consistent with the unique functional groups (chlorovinylidene group and terminal vinyl chloride) present in *T. thiebautii* metabolites (although these functional groups were not in **1**) and genetic architecture consistent with putative PKS-NRPS-derived metabolite, e.g., tricholides A and B and **1**. We also examined genomes and MAGs from *T. thiebautii* and *T. erythraeum* for putative full biosynthetic gene clusters (BGCs) that might include **1**. Specifically, this included the genomes of *T. thiebautii* H94, *T. erythraeum* IMS101, and the metagenome assemblies obtained from samples collected during the R/V Atlantis TriCoLim cruise,[25] having some colocation with the archived samples from the cruise that we analyzed chemically during this work. Analysis of PKS clusters present in the *T. thiebautii* H94 genome using the antiSMASH platform[40] and the known cluster BLAST function identified a module in the *T. thiebautii* H94 genome, which showed similarity to modules in the curacin A pathway.[41] Curacin A possesses a terminal alkene functionality and the biochemistry surrounding its construction, and the activity of the decarboxylating thioesterase has been experimentally shown.[42] Additional mining and annotation using DELTA-BLAST[43] showed the presence of the following domains in the *T. thiebautii* cluster of interest: ketosynthase (KS), acyltransferase (AT), ketoreductase (KR), acyl carrier protein (ACP), sulfotransferase (ST), and a thioesterase domain (TE). These domains are consistent with those that form the terminal alkene in curacin A.[41] Furthermore, adjacent to this module was a gene that BLAST searching annotated as an Fe(II)-dependent halogenase. This partial cluster was similar to the genes predicted to form the terminal vinyl chloride in many of the trichophycins and trichothiazole (Figure S25A). A second partial gene cluster showed remarkable consistency with the genetic architecture necessary to form the chlorovinylidene group. An HCS cassette was present in this cluster consisting of an HMG-CoA synthase and two enoyl CoA hydratases and ketosynthase, acyltransferase, and three ACP domains with additional enoyl reductase and ketosynthase domains (Figure S25B). The HCS cassette has been observed in gene clusters that produce products with the chlorovinylidene moiety, such as the jamaicamide biosynthetic pathway.[44] While a specific halogenase was not identified in this partial cluster, the elements are present for the vinylidene group observed in nearly all the metabolites isolated from *T. thiebautii* collections (Figure S4). The HMG-CoA synthase was also identified in MAGs Bin1_Station19 and Bin1_Station18, which phylogenomics analysis supported as *T. thiebautii*.[25] We predict that a PKS-NRPS system that generates **1** and one of the NRPS modules would have a cyclization domain to create the thiazole. Additionally, we predict that this gene cluster would have

https://doi.org/10.1021/acs.est.3c10739
Environ. Sci. Technol. 2024, 58, 9525−9535

several methyltransferases including an *N*-methyl transferase. However, no cluster was consistent with these predictions in any genome examined and we could not identify the putative gene cluster that creates trichothilone A (**1**).

DISCUSSION

***Trichodesmium* Species as Toxin and Specialized Metabolite Producers.** With the occurrence of cyanobacterial blooms increasing concurrent with climatological changes, there is a need to determine the ecological role of specialized metabolites and how they affect speciation, ecotoxicology, and range expansion. The rarity of *Trichodesmium* cultures stems from an inability for most laboratories to obtain hand samples and to scale up cultures of *Trichodesmium* for the biomass amounts that can lead to the isolation of metabolites. This has necessitated that many toxin and specialized metabolite isolation efforts come from environmental collections. While many classes of metabolites have been detected from these blooms, it is difficult to attribute production of these metabolites, including **1**, to *Trichodesmium* without analysis of axenic cultures. However, the widespread presence of **1** in environmental collections and its detection in three independent unialgal cultures of *Trichodesmium* supports its cyanobacterial production, and its presence in the media may indicate an important ecological role. The *T. thiebautii*-dominated blooms and collected colonies showed intriguing profiles with respect to their metabolite composition. Continuing longitudinal and geographic studies will aid in understanding the metabolite profiles of this group and potentially lead to understanding the ecological role of these metabolites. The widespread presence of trichothiazole, trichothilone A (**1**), and other metabolites presumes that they likely have an important physiological or ecological role. Additionally, the widespread presence of smenamides A/B and smenothiazole A warrant a reinvestigation of *Trichodesmium* toxicity, as these metabolites showed cytotoxic effects to human cells at nanomolar concentrations.[17,18] While the trichophycins, trichothiazoles, tricholides, and other metabolites we have isolated from *T. thiebautii* have shown toxicity to human cells generally at low micromolar levels,[13−19] it is important to consider the additive or synergistic effect of toxin mixtures. We have established a demonstrated analytical capability to show that certain specialized metabolites are found in colonies in the GoM and the wider Caribbean and Atlantic Ocean, but *Trichodesmium* is found around the globe with notable repeated blooms in the Pacific and Indian Oceans.[45] It would be most interesting to continue analysis in collections from these areas using our established methods to provide further foundational studies on *Trichodesmium*-specialized metabolism. The ability to accumulate more material from yearly blooms will enhance the potential for **1** and other metabolites to be comprehensively evaluated for their potential therapeutic benefit and ecological function. Furthermore, there remain hundreds of uncharacterized metabolites as shown in the various molecular networks we have generated. We are only scratching the surface of the molecular potential of *Trichodesmium*.

Connecting Biosynthetic Pathways to *Trichodesmium*-Specialized Metabolites. Field samples are more accurately defined in a clade format dominated by one of the two major groups of *Trichodesmium* (*T. erythraeum* or *T. thiebautii*), and recent work has shown that there are four clades of N_2-fixing *Trichodesmium* (*T. erythraeum* A and B, *T. thiebautii* A and B).[25] Until there is an unequivocal biosynthetic identification of complete gene clusters in the *T. thiebautii* genomes, and the lack of these clusters in strains of *T. erythraeum*, no definitive answer can be given on species chemotaxonomy and metabologenomics. There is also previously published evidence that indicates environment populations are composed of mixed species.[46] Defining species assemblages in collections will be necessary to understand community composition and how this may affect specialized metabolite production. Furthermore, while the cultivated sample of *T. erythraeum* only showed the presence of one of the specialized metabolites we have characterized (**1**), the culture conditions may not be conducive to metabolite production, or we do not understand the environmental triggers necessary for metabolite expression. While dozens of molecules have been characterized from *Trichodesmium* by our group, they have similar carbon scaffolds and most are analogues of each other. We speculate that the biosynthesis of these products in *Trichodesmium* follows that deciphered for the vatiamides in which a unique combinatorial nonlinear hybrid PKS-NRPS system generated a series of analogues adding to molecular diversity.[47]

Holistic molecular approaches must be taken to define species assemblages, genomic analysis to define biosynthetic architecture, and culture and field experiments to understand potential abiotic and biotic triggers that control metabolite production. Additionally, as the bulk of these samples were from field collections, there are many variables such as the impact of the bacterial and microbial community and the sample volumes collected vary widely from a few colonies to bulk collections. Instituting water volume measures, colony counts, and more molecular community data will aid in better detection and more comparable data across samples. Untargeted LC-MS/MS networking has shown utility in the discovery of new cyanobacterial toxins and metabolites previously,[48] and it was well tailored for the present study. Recent work has shown that along the West Florida Shelf, there is a coastal vs open ocean separation for *T. erythraeum* and *T. thiebautii*, respectively.[49] It would be most interesting to investigate if specialized metabolism plays a role in this niche differentiation. The discovery of a nondiazotrophic *Trichodesmium* species[50] provokes additional questions with respect to comparative metabolomics studies and the potential role of specialized metabolites in nitrogen fixation. Understanding how potential abiotic stressors regulate specialized metabolite and protein production will be key in determining the ecological role of the molecules we have discovered.[51] *Trichodesmium*'s iron uptake is well studied, and the impact of specialized metabolites on iron bioavailability in the phycosphere[52] should be an area of further study to fully understand the ecophysiological role of these specialized metabolites.

ASSOCIATED CONTENT

Supporting Information

The Supporting Information is available free of charge at https://pubs.acs.org/doi/10.1021/acs.est.3c10739.

Experimental details and analytical and genomic data (PDF)

Metabolites annotations at sampling stations (XLSX)

Isotropic shieldings for each conformer for computations (XLSX)

https://doi.org/10.1021/acs.est.3c10739
Environ. Sci. Technol. 2024, 58, 9525−9535

AUTHOR INFORMATION

Corresponding Authors

Alfonso Mangoni − *Dipartimento di Farmacia, Università degli Studi di Napoli Federico II, Napoli 80131, Italy;* orcid.org/0000-0003-3910-6518; Email: alfonso.mangoni@unina.it

Matthew J. Bertin − *Department of Chemistry, Case Western Reserve University, Cleveland, Ohio 44106, United States;* orcid.org/0000-0002-2200-0277; Email: mxb1224@case.edu

Authors

Christopher W. Via − *Department of Biomedical and Pharmaceutical Sciences, College of Pharmacy, University of Rhode Island, Kingston, Rhode Island 02881, United States*

Laura Grauso − *Dipartimento di Agraria, Università degli Studi di Napoli Federico II, Portici Napoli 80055, Italy*

Kelly M. McManus − *Department of Biomedical and Pharmaceutical Sciences, College of Pharmacy, University of Rhode Island, Kingston, Rhode Island 02881, United States*

Riley D. Kirk − *Department of Biomedical and Pharmaceutical Sciences, College of Pharmacy, University of Rhode Island, Kingston, Rhode Island 02881, United States*

Andrew M. Kim − *Department of Biomedical and Pharmaceutical Sciences, College of Pharmacy, University of Rhode Island, Kingston, Rhode Island 02881, United States*

Eric A. Webb − *Marine and Environmental Biology, Department of Biological Sciences, University of Southern California, Los Angeles, California 90089, United States*

Noelle A. Held − *Marine and Environmental Biology, Department of Biological Sciences, University of Southern California, Los Angeles, California 90089, United States*

Mak A. Saito − *Department of Marine Chemistry and Geochemistry, Woods Hole Oceanographic Institution, Woods Hole, Massachusetts 02543, United States;* orcid.org/0000-0001-6040-9295

Silvia Scarpato − *Dipartimento di Farmacia, Università degli Studi di Napoli Federico II, Napoli 80131, Italy*

Paul V. Zimba − *Rice Rivers Center, Virginia Commonwealth University, Richmond, Virginia 23284, United States*

Peter D. R. Moeller − *Harmful Algal Bloom Monitoring and Reference Branch, Stressor Detection and Impacts Division, National Ocean Service/NOAA, Hollings Marine Laboratory, Charleston, South Carolina 29412, United States*

Complete contact information is available at: https://pubs.acs.org/10.1021/acs.est.3c10739

Author Contributions

◆C.W.V. and L.G. contributed equally.

Author Contributions

M.J.B. and A.M. conceived the study and performed analysis. C.W.V., L.G., K.M.M., R.D.K., A.M.K., and S.S. performed data acquisition and analysis. E.A.W., N.A.H., M.A.S., P.V.Z., and P.D.R.M. provided key samples and data interpretation. The manuscript was written through contributions of all authors. All authors have given approval to the final version of the manuscript. C.W.V. and L.G. contributed equally.

Funding

Acquisition of certain data in this publication was made possible by the use of equipment and services available through grant number P20GM103430. We also gratefully acknowledge support from NSF-2125191 to M.A.S. and E.A.W. Research reported in this article was supported in part by the National Institute of Environmental Health Sciences of the National Institutes of Health under Award Number R21ES033758 (M.J.B.) and the American Society of Pharmacognosy Starter Grant (M.J.B).

Notes

The authors declare no competing financial interest.

ACKNOWLEDGMENTS

We profusely thank Dr. Simon J. Geist at Texas A&M, Corpus Christi, for assistance with collections. We gratefully acknowledge the crew of the Oregon II and NOAA with special thanks to Andrew Millett and Glenn Zapfe. The Table of Contents Graphic and Figure S1 were created in part with Biorender.com (agreement #XL26T0KI8K and # WU26T0KYIN, respectively).

ABBREVIATIONS

BGC, biosynthetic gene cluster; DAD, diode array detector; DFT, density functional theory; ESI, electrospray ionization; GNPS, Global Natural Product Social Molecular Networking; GoM, Gulf of Mexico; HRMS, high-resolution mass spectrometry; LC-MS/MS, liquid chromatography-tandem mass spectrometry; MAG, metagenome-assembled genome; MTPA-Cl, α-methoxy-α-(trifluoromethyl)phenylacetyl chloride; NMR, nuclear magnetic resonance; PKS-NRPS, polyketide synthase-nonribosomal peptide synthetase; USCTCC, University of Southern California *Trichodesmium* Culture Collection

REFERENCES

(1) Hutchins, D. A.; Fu, F.-X.; Webb, E. A.; Walworth, N.; Tagliabue, A. Taxon-Specific Response of Marine Nitrogen Fixers to Elevated Carbon Dioxide Concentrations. *Nature Geosci* **2013**, *6* (9), 790−795.

(2) Hutchins, D. A.; Walworth, N. G.; Webb, E. A.; Saito, M. A.; Moran, D.; McIlvin, M. R.; Gale, J.; Fu, F.-X. Irreversibly Increased Nitrogen Fixation in *Trichodesmium* Experimentally Adapted to Elevated Carbon Dioxide. *Nat. Commun.* **2015**, *6* (1), 8155.

(3) Boatman, T. G.; Lawson, T.; Geider, R. J. A Key Marine Diazotroph in a Changing Ocean: The Interacting Effects of Temperature, CO2 and Light on the Growth of *Trichodesmium erythraeum* IMS101. *PLoS One* **2017**, *12* (1), No. e0168796.

(4) Sacilotto Detoni, A. M.; Fonseca Costa, L. D.; Pacheco, L. A.; Yunes, J. S. Toxic *Trichodesmium* Bloom Occurrence in the Southwestern South Atlantic Ocean. *Toxicon* **2016**, *110*, 51−55.

(5) Shunmugam, S.; Gayathri, M.; Prasannabalaji, N.; Thajuddin, N.; Muralitharan, G. Unraveling the Presence of Multi-Class Toxins from *Trichodesmium* Bloom in the Gulf of Mannar Region of the Bay of Bengal. *Toxicon* **2017**, *135*, 43−50.

(6) Ramos, A.; Martel, A.; Codd, G.; Soler, E.; Coca, J.; Redondo, A.; Morrison, L.; Metcalf, J.; Ojeda, A.; Suárez, S.; Petit, M. Bloom of the Marine Diazotrophic Cyanobacterium *Trichodesmium erythraeum* in the Northwest African Upwelling. *Mar. Ecol.: Prog. Ser.* **2005**, *301*, 303−305.

(7) Kerbrat, A. S.; Amzil, Z.; Pawlowiez, R.; Golubic, S.; Sibat, M.; Darius, H. T.; Chinain, M.; Laurent, D. First Evidence of palytoxin and 42-Hydroxy-palytoxin in the Marine Cyanobacterium *Trichodesmium*. *Marine Drugs* **2011**, *9* (4), 543−560.

(8) Sudek, S.; Haygood, M. G.; Youssef, D. T. A.; Schmidt, E. W. Structure of trichamide, a Cyclic Peptide from the Bloom-Forming Cyanobacterium *Trichodesmium erythraeum*, Predicted from the Genome Sequence. *Appl. Environ. Microbiol.* **2006**, *72* (6), 4382−4387.

(9) Hawser, S. P.; O'Neil, J. M.; Roman, M. R.; Codd, G. A. Toxicity of Blooms of the Cyanobacterium *Trichodesmium* to Zooplankton. *J. Appl. Phycol* **1992**, *4* (1), 79−86.

(10) Guo, C.; Tester, P. A. Toxic Effect of the Bloom-Forming *Trichodesmium* sp. (Cyanophyta) to the copepod *Acartia tonsa*. *Nat. Toxins* **1994**, *2* (4), 222−227.

(11) Narayana, S.; Chitra, J.; Tapase, S. R.; Thamke, V.; Karthick, P.; Ramesh, Ch.; Murthy, K. N.; Ramasamy, M.; Kodam, K. M.; Mohanraju, R. Toxicity Studies of *Trichodesmium erythraeum* (Ehrenberg, 1830) Bloom Extracts, from Phoenix Bay, Port Blair, Andamans. *Harmful Algae* **2014**, *40*, 34−39.
(12) Via, C. W.; Glukhov, E.; Costa, S.; Zimba, P. V.; Moeller, P. D. R.; Gerwick, W. H.; Bertin, M. J. The Metabolome of a Cyanobacterial Bloom Visualized by MS/MS-Based Molecular Networking Reveals New Neurotoxic Smenamide Analogs (C, D, and E). *Front. Chem.* **2018**, 316 DOI: 10.3389/fchem.2018.00316.
(13) Bertin, M. J.; Wahome, P. G.; Zimba, P. V.; He, H.; Moeller, P. D. R. Trichophycin A, a Cytotoxic Linear Polyketide Isolated from a *Trichodesmium thiebautii* Bloom. *Mar. Drugs* **2017**, *15*, 10 DOI: 10.3390/md15010010.
(14) Bertin, M. J.; Saurí, J.; Liu, Y.; Via, C. W.; Roduit, A. F.; Williamson, R. T. Trichophycins B-F, Chlorovinylidene-containing Polyketides Isolated from a Cyanobacterial Bloom. *J. Org. Chem.* **2018**, *83*, 13256−13266.
(15) Bertin, M. J.; Roduit, A. F.; Sun, J.; Alves, G. E.; Via, C. W.; Gonzalez, M. A.; Zimba, P. V.; Moeller, P. D. R. tricholides A and B and Unnarmicin D: New Hybrid PKS-NRPS Macrocycles Isolated from an Environmental Collection of *Trichodesmium thiebautii*. *Mar. Drugs* **2017**, *15*, 206 DOI: 10.3390/md15070206.
(16) Belisle, R. S.; Via, C. W.; Schock, T. B.; Villareal, T. A.; Zimba, P. V.; Beauchesne, K. R.; Moeller, P. D. R.; Bertin, M. J. Trichothiazole A, a Dichlorinated Polyketide Containing an Embedded thiazole Isolated from *Trichodesmium* Blooms. *Tetrahedron Lett.* **2017**, *58*, 4066−4068.
(17) Teta, R.; Irollo, E.; Della Sala, G.; Pirozzi, G.; Mangoni, A.; Costantino, V. smenamides A and B, Chlorinated Peptide/Polyketide Hybrids Containing a Dolapyrrolidinone Unit from the Caribbean Sponge *Smenospongia aurea*. Evaluation of Their Role as Leads in Antitumor Drug Research. *Marine Drugs* **2013**, *11* (11), 4451−4463.
(18) Esposito, G.; Teta, R.; Miceli, R.; Ceccarelli, L.; Della Sala, G.; Camerlingo, R.; Irollo, E.; Mangoni, A.; Pirozzi, G.; Costantino, V. Isolation and Assessment of the in Vitro Anti-Tumor Activity of smenothiazole A and B, Chlorinated thiazole-Containing Peptide/Polyketides from the Caribbean Sponge. *Smenospongia aurea. Marine Drugs* **2015**, *13* (1), 444−459.
(19) Bertin, M. J.; Zimba, P. V.; He, H.; Moeller, P. D. R. Structure Revision of Trichotoxin, a Chlorinated Polyketide Isolated from a *Trichodesmium thiebautii* Bloom. *Tetrahedron Lett.* **2016**, *57*, 5864−5867.
(20) Caso, A.; Esposito, G.; Della Sala, G.; Pawlik, J. R.; Teta, R.; Mangoni, A.; Costantino, V. Fast Detection of Two Smenamide Family Members Using Molecular Networking. *Marine Drugs* **2019**, *17* (11), 618.
(21) Esposito, G.; Della Sala, G.; Teta, R.; Caso, A.; Bourguet-Kondracki, M.; Pawlik, J. R.; Mangoni, A.; Costantino, V. Chlorinated thiazole-Containing Polyketide-Peptides from the Caribbean Sponge *Smenospongia conulosa*: Structure Elucidation on Microgram Scale. *Eur. J. Org. Chem.* **2016**, *2016* (16), 2871−2875.
(22) Teta, R.; Della Sala, G.; Esposito, G.; Via, C. W.; Mazzoccoli, C.; Piccoli, C.; Bertin, M. J.; Costantino, V.; Mangoni, A. A Joint Molecular Networking Study of a *Smenospongia* Sponge and a Cyanobacterial Bloom Revealed New Antiproliferative Chlorinated Polyketides. *Org. Chem. Front.* **2019**, *6*, 1762−1774.
(23) McManus, K. M.; Kirk, R. D.; Via, C. W.; Lotti, J. S.; Roduit, A. F.; Teta, R.; Scarpato, S.; Mangoni, A.; Bertin, M. J. Isolation of Isotrichophycin C and Trichophycins G−I from a Collection of *Trichodesmium thiebautii*. *J. Nat. Prod.* **2020**, *83* (9), 2664−2671.
(24) Komárek, J; Anagnostidis, K. *Cyanoprokarota Part 2: Oscillatoriales, Freshwater Flora of Central Europe*; Spektrum Akademischer Verlag: Heidelberg, Germany, 2007. pp 1- 759.
(25) Webb, E. A.; Held, N. A.; Zhao, Y.; Graham, E. D.; Conover, A. E.; Semones, J.; Lee, M. D.; Feng, Y.; Fu, F.; Saito, M. A.; Hutchins, D. A. Importance of Mobile Genetic Element Immunity in Numerically Abundant *Trichodesmium* Clades. *ISME Commun.* **2023**, *3* (1), 15.
(26) Wang, M.; Carver, J. J.; Phelan, V. V.; Sanchez, L. M.; Garg, N.; Peng, Y.; Nguyen, D. D.; Watrous, J.; Kapono, C. A.; Luzzatto-Knaan, T.; Porto, C.; Bouslimani, A.; Melnik, A. V.; Meehan, M. J.; Liu, W.-T.; Crüsemann, M.; Boudreau, P. D.; Esquenazi, E.; Sandoval-Calderón, M.; Kersten, R. D.; Pace, L. A.; Quinn, R. A.; Duncan, K. R.; Hsu, C.-C.; Floros, D. J.; Gavilan, R. G.; Kleigrewe, K.; Northen, T.; Dutton, R. J.; Parrot, D.; Carlson, E. E.; Aigle, B.; Michelsen, C. F.; Jelsbak, L.; Sohlenkamp, C.; Pevzner, P.; Edlund, A.; McLean, J.; Piel, J.; Murphy, B. T.; Gerwick, L.; Liaw, C.-C.; Yang, Y.-L.; Humpf, H.-U.; Maansson, M.; Keyzers, R. A.; Sims, A. C.; Johnson, A. R.; Sidebottom, A. M.; Sedio, B. E.; Klitgaard, A.; Larson, C. B.; Boya, P. C. A.; Torres-Mendoza, D.; Gonzalez, D. J.; Silva, D. B.; Marques, L. M.; Demarque, D. P.; Pociute, E.; O'Neill, E. C.; Briand, E.; Helfrich, E. J. N.; Granatosky, E. A.; Glukhov, E.; Ryffel, F.; Houson, H.; Mohimani, H.; Kharbush, J. J.; Zeng, Y.; Vorholt, J. A.; Kurita, K. L.; Charusanti, P.; McPhail, K. L.; Nielsen, K. F.; Vuong, L.; Elfeki, M.; Traxler, M. F.; Engene, N.; Koyama, N.; Vining, O. B.; Baric, R.; Silva, R. R.; Mascuch, S. J.; Tomasi, S.; Jenkins, S.; Macherla, V.; Hoffman, T.; Agarwal, V.; Williams, P. G.; Dai, J.; Neupane, R.; Gurr, J.; Rodríguez, A. M. C.; Lamsa, A.; Zhang, C.; Dorrestein, K.; Duggan, B. M.; Almaliti, J.; Allard, P.-M.; Phapale, P.; Nothias, L.-F.; Alexandrov, T.; Litaudon, M.; Wolfender, J.-L.; Kyle, J. E.; Metz, T. O.; Peryea, T.; Nguyen, D.-T.; VanLeer, D.; Shinn, P.; Jadhav, A.; Müller, R.; Waters, K. M.; Shi, W.; Liu, X.; Zhang, L.; Knight, R.; Jensen, P. R.; Palsson, B. Ø.; Pogliano, K.; Linington, R. G.; Gutiérrez, M.; Lopes, N. P.; Gerwick, W. H.; Moore, B. S.; Dorrestein, P. C.; Bandeira, N. Sharing and Community Curation of Mass Spectrometry Data with Global Natural Products Social Molecular Networking. *Nat. Biotechnol.* **2016**, *34* (8), 828−837.
(27) Matsumori, N.; Kaneno, D.; Murata, M.; Nakamura, H.; Tachibana, K. Stereochemical Determination of Acyclic Structures Based on Carbon−Proton Spin-Coupling Constants. A Method of Configuration Analysis for Natural Products. *J. Org. Chem.* **1999**, *64* (3), 866−876.
(28) Koźmiński, W.; Nanz, D. *J. Magn. Reson.* **2000**, *142* (2), 294−299.
(29) Ciminiello, P.; Dell'Aversano, C.; Dello Iacovo, E.; Fattorusso, E.; Forino, M.; Grauso, L.; Tartaglione, L. *Eur. J. Chem.* **2012**, *18* (52), 16836−16843.
(30) Kobayashi, Y.; Lee, J.; Tezuka, K.; Kishi, Y. Toward Creation of a Universal NMR Database for the Stereochemical Assignment of Acyclic Compounds: The Case of Two Contiguous Propionate Units. *Org. Lett.* **1999**, *1* (13), 2177−2180.
(31) Lee, J.; Kobayashi, Y.; Tezuka, K.; Kishi, Y. Toward Creation of a Universal NMR Database for the Stereochemical Assignment of Acyclic Compounds: Proof of Concept. *Org. Lett.* **1999**, *1* (13), 2181−2184.
(32) Grauso, L.; Li, Y.; Scarpato, S.; Cacciola, N. A.; De Cicco, P.; Zidorn, C.; Mangoni, A. A Cytotoxic Heterodimeric Cyclic Diarylheptanoid with a Rearranged Benzene Ring from the Seagrass Zostera Marina. *J. Nat. Prod.* **2022**, *85* (10), 2468−2473.
(33) Scarpato, S.; Teta, R.; De Cicco, P.; Borrelli, F.; Pawlik, J. R.; Costantino, V.; Mangoni, A. Molecular Networking Revealed Unique UV-Absorbing Phospholipids: Favilipids from the Marine Sponge *Clathria faviformis*. *Mar. Drugs* **2023**, *21* (2), 58.
(34) Gilbert, K. E. *Pcmodel (version 10.0)*; Serena Software: Bloomington, IN, 2013.
(35) *Gaussian 16*, Revision C.01; Gaussian Inc.: Wallingford CT, USA.
(36) Grimblat, N.; Zanardi, M. M.; Sarotti, A. M. Beyond DP4: An Improved Probability for the Stereochemical Assignment of Isomeric Compounds Using Quantum Chemical Calculations of NMR Shifts. *J. Org. Chem.* **2015**, *80* (24), 12526−12534.
(37) Schmidt, Y.; Lehr, K.; Colas, L.; Breit, B. Assignment of relative Configuration of Desoxypropionates by ^{1}H NMR Spectroscopy: Method Development, Proof of Principle by Asymmetric Total Synthesis of Xylarinic Acid A and Applications. *Chem.—Eur. J.* **2012**, *18*, 7071−7081.
(38) Bodo, B.; Trowitzsch-Kienast, W.; Schomburg, D. Absolute Configuration of Bourgeanic Acid: X-Ray Crystal Structure of a 4-Bromophenacyl Derivative of Hemibourgeanic Acid. *Tetrahedron Lett.* **1986**, *27* (7), 847−848.

(39) Steinmetz, H.; Irschik, H.; Kunze, B.; Reichenbach, H.; Höfle, G.; Jansen, R. thuggacins, Macrolide Antibiotics Active against *Mycobacterium Tuberculosis*: Isolation from Myxobacteria, Structure Elucidation, Conformation Analysis and Biosynthesis. *Chem.—Eur. J.* **2007**, *13* (20), 5822−5832.
(40) Blin, K.; Shaw, S.; Kloosterman, A. M.; Charlop-Powers, Z.; van Wezel, G. P.; Medema, M. H.; Weber, T. AntiSMASH 6.0: Improving Cluster Detection and Comparison Capabilities. *Nucleic Acids Res.* **2021**, *49* (W1), W29−W35.
(41) Chang, Z.; Sitachitta, N.; Rossi, J. V.; Roberts, M. A.; Flatt, P. M.; Jia, J.; Sherman, D. H.; Gerwick, W. H. Biosynthetic Pathway and Gene Cluster Analysis of Curacin A, an Antitubulin Natural Product from the Tropical Marine Cyanobacterium *Lyngbya majuscula*. *J. Nat. Prod.* **2004**, *67* (8), 1356−1367.
(42) Gehret, J. J.; Gu, L.; Gerwick, W. H.; Wipf, P.; Sherman, D. H.; Smith, J. L. Terminal alkene Formation by the thioesterase of Curacin A Biosynthesis. *J. Biol. Chem.* **2011**, *286* (16), 14445−14454.
(43) Boratyn, G. M.; Schäffer, A. A.; Agarwala, R.; Altschul, S. F.; Lipman, D. J.; Madden, T. L. Domain Enhanced Lookup Time Accelerated BLAST. *Biol. Direct* **2012**, *7* (1), 12.
(44) Edwards, D. J.; Marquez, B. L.; Nogle, L. M.; McPhail, K.; Goeger, D. E.; Roberts, M. A.; Gerwick, W. H. Structure and Biosynthesis of the Jamaicamides, New Mixed Polyketide-Peptide Neurotoxins from the Marine Cyanobacterium *Lyngbya majuscula*. *Chem. Biol.* **2004**, *11* (6), 817−833.
(45) Bergman, B.; Sandh, G.; Lin, S.; Larsson, J.; Carpenter, E. J. *Trichodesmium* − a widespread marine cyanobacterium with unusual nitrogen fixation properties. *FEMS Microbiol. Rev.* **2013**, *37*, 286−302.
(46) Hynes, A. M.; Webb, E. A.; Doney, S. C.; Waterbury, J. B. Comparison of Cultured *Trichodesmium* (Cyanophyceae) with Species Characterized from the Field. *Journal of Phycology* **2012**, *48* (1), 196−210.
(47) Moss, N. A.; Seiler, G.; Leão, T. F.; Castro-Falcón, G.; Gerwick, L.; Hughes, C. C.; Gerwick, W. H. Nature's Combinatorial Biosynthesis Produces vatiamides A−F. *Angew. Chem., Int. Ed.* **2019**, *58* (27), 9027−9031.
(48) Teta, R.; Della Sala, G.; Glukhov, E.; Gerwick, L.; Gerwick, W. H.; Mangoni, A.; Costantino, V. Combined LC−MS/MS and Molecular Networking Approach Reveals New Cyanotoxins from the 2014 Cyanobacterial Bloom in Green Lake, Seattle. *Environ. Sci. Technol.* **2015**, *49* (24), 14301−14310.
(49) Confesor, K. A.; Selden, C. R.; Powell, K. E.; Donahue, L. A.; Mellett, T.; Caprara, S.; Knapp, A. N.; Buck, K. N.; Chappell, P. D. Defining the Realized Niche of the Two Major Clades of *Trichodesmium*: A Study on the West Florida Shelf. *Front. Mar. Sci.* **2022**, *9*, No. 821655, DOI: 10.3389/fmars.2022.821655.
(50) Delmont, T. O. Discovery of nondiazotrophic *Trichodesmium* species abundant and widespread in the open ocean. *Proc. Natl. Acad. Sci. U. S. A.* **2021**, *118* (46), No. e2112355118.
(51) Held, N. A.; Webb, E. A.; McIlvin, M. M.; Hutchins, D. A.; Cohen, N. R.; Moran, D. M.; Kunde, K.; Lohan, M. C.; Mahaffey, C.; Woodward, E. M. S.; Saito, M. A. Co-Occurrence of Fe and P Stress in Natural Populations of the Marine Diazotroph *Trichodesmium*. *Biogeosciences* **2020**, *17* (9), 2537−2551.
(52) Liu, F.; Tan, Q.-G.; Weiss, D.; Crémazy, A.; Fortin, C.; Campbell, P. G. C. Unravelling Metal Speciation in the Microenvironment Surrounding Phytoplankton Cells to Improve Predictions of Metal Bioavailability. *Environ. Sci. Technol.* **2020**, *54* (13), 8177−8185.

https://doi.org/10.1021/acs.est.3c10739
Environ. Sci. Technol. 2024, 58, 9525−9535